

## Recent advances in resonant-tunneling-diode oscillators

E.R. Brown, C.D. Parker, K.M. Molvar, and M.K. Connors  
*Lincoln Laboratory, Massachusetts Institute of Technology*  
*Lexington, MA 02173-9108*

K.D. Stephan

*Department of Electrical and Computer Engineering, University of Massachusetts*  
*Amherst, MA 01003*

### Abstract

Oscillation frequencies between 100 and 712 GHz have been obtained in InAs/AlSb double-barrier resonant-tunneling diodes (RTDs). The power density obtained at 360 GHz was  $90 \text{ W cm}^{-2}$ , which is 50 times that obtained from GaAs/AlAs diodes at essentially the same frequency. Oscillation at 712 GHz with a power of  $0.3 \mu\text{W}$  was observed, representing the highest oscillation frequency reported to date from a solid-state electronic oscillator at room temperature. A high-Q semiconfocal resonator has been used to lock a waveguide-resonator-based RTD oscillator operating at a frequency of 103 GHz. The locked-oscillator linewidth was 40 kHz, which is about 250 times narrower than the linewidth of the oscillator without the high-Q resonator.

### Introduction

The double-barrier resonant-tunneling diode (RTD) has demonstrated promising high-speed characteristics as an oscillator and a switch. Until recently, most of the high-speed experiments have been conducted with RTDs made from the GaAs/AlAs material system (GaAs quantum well and cladding layers, AlAs barriers). Oscillators made from such diodes have operated at room temperature up to 420 GHz.<sup>1</sup> It has been shown that the maximum oscillation frequency of GaAs/AlAs RTDs,  $f_{\text{max}}$ , is limited by a high series resistance  $R_S$  and a low magnitude of differential conductance  $G$  in the negative differential conductance (NDC) region.

These shortcomings are alleviated in RTDs made from the indium-bearing material systems,  $\text{In}_{0.53}\text{Ga}_{0.47}\text{As}/\text{AlAs}$ <sup>2</sup> and  $\text{InAs}/\text{AlSb}$ .<sup>3</sup> The indium-bearing RTDs provide a lower  $R_S$  primarily because ohmic contacts on  $\text{In}_{0.53}\text{Ga}_{0.47}\text{As}$  and  $\text{InAs}$  have lower resistance than on GaAs. In addition, indium-bearing RTDs provide a higher magnitude of  $G$  because of the larger available current density  $\Delta J$  in the NDC region, where  $\Delta J = J_P - J_V$ , and  $J_P$  and  $J_V$  are the peak and valley current densities, respectively. The indium-bearing materials also increase  $f_{\text{max}}$  by reducing the transit-time delay per unit depletion length on the anode side of the double-barrier structure.

Our indium-bearing RTDs are all grown by molecular-beam epitaxy. The  $\text{In}_{0.53}\text{Ga}_{0.47}\text{As}/\text{AlAs}$  RTDs were grown on InP substrates, and the  $\text{InAs}/\text{AlSb}$  RTDs were grown on GaAs and InAs substrates. The current-voltage (I-V) curve of our fastest  $\text{InAs}/\text{AlSb}$  RTD tested to date is shown in Fig. 1. It has a peak-to-valley current ratio of about 3.4 at room temperature, and a peak current density of  $2.8 \times 10^5 \text{ A cm}^{-2}$ , corresponding to  $\Delta J \cong 2.0 \times 10^5 \text{ A cm}^{-2}$ . It consists of two 1.5-nm-thick undoped AlSb barriers separated by a 6.4-nm-thick undoped InAs quantum well. Below the double-barrier structure are a 75-nm-thick InAs layer doped to  $N_D \cong 2 \times 10^{17} \text{ cm}^{-3}$ , a 0.2- $\mu\text{m}$  InAs layer doped to  $N_D = 2 \times 10^{18} \text{ cm}^{-3}$ , and a 0.5- $\mu\text{m}$  layer doped to  $N_D = 5 \times 10^{18} \text{ cm}^{-3}$ . The former layer is designed to be fully depleted under bias. Above the double-barrier structure is a 10-nm-thick undoped InAs buffer layer, a 100-nm-thick InAs layer doped to  $N_D = 2 \times 10^{18} \text{ cm}^{-3}$ , a 100-nm-thick InAs layer doped to  $N_D = 5 \times 10^{18} \text{ cm}^{-3}$ , and a 20-nm-thick indium layer. The indium layer forms an *in situ* nonalloyed ohmic contact, as shown in the cross-sectional view in Fig. 2. The procedures used to fabricate the diode mesas are described in Ref. 3.

### High-frequency chips

With RTDs intended for high-frequency oscillators, it is important to achieve a low-resistance current path from the active region of the device to the ground plane. For diodes to be tested in waveguide circuits, the low resistance is achieved in the manner shown in Fig. 2. The diode mesas are isolated by chemically etching to the top of an  $n^+$  epilayer that is doped to a concentration of  $N_D \geq 5 \times 10^{18} \text{ cm}^{-3}$ . The wafer is then diced into small ( $100 \times 100 \mu\text{m}$ ) chips, and the sidewalls are metallized with a thin layer of electroless palladium and a thicker layer of electroplated gold. This yields a typical series resistance from the double-barrier structure to the bottom of the chip of  $0.5 \Omega$  at dc, increasing to about  $1.0 \Omega$  at 600 GHz.

It is also important with high-frequency chips to make low-resistance and stable whisker contacts. This was accomplished by fabricating the surface of the wafer into a honeycomb structure, as shown in Fig. 3. The honeycomb topology is produced by first plasma depositing approximately  $1 \mu\text{m}$  of  $\text{Si}_3\text{N}_4$  at a temperature of  $200 \text{ }^\circ\text{C}$ . The  $\text{Si}_3\text{N}_4$  is patterned with photoresist, and via holes extending down to the top of the mesas are opened by reactive-ion etching. In addition, the  $\text{Si}_3\text{N}_4$  is a passivation layer for InGaAs alloys,<sup>4</sup> so the RTDs should operate under a number of adverse conditions.

### Oscillator measurements

After fabrication the chips are mounted in one of four full-height rectangular waveguide resonators operating in frequency bands around 100, 200, 400, and 650 GHz, respectively. The design of these resonators is shown in Fig. 4. In each case, the RTD chip is mounted below a post that extends roughly halfway into the waveguide. The combination of the capacitance of the gap below the post and the inductance of the whisker create an LC resonance that is the basis for the oscillation in these waveguide structures. The highest frequency resonator constructed to date consists of a  $0.015 \times 0.030\text{-cm}$  (WR-1) full-height rectangular

waveguide with a contacting backshort.

Up to 400 GHz, the power of the oscillations is measured by waveguide-mounted Schottky-diode detectors. The frequency is measured by wavemeters or by down-conversion techniques. Above 600 GHz, the power is measured by coupling the radiation out of the waveguide with a pyramidal feedhorn and focusing it onto a composite bolometer. This bolometer consists of a silicon thermistor element bonded to a  $377\text{-}\Omega/\square$  absorber. The absorber is mounted in a hemispherical integrating cavity. The oscillation frequency is measured by placing a scanning Fabry-Perot spectrometer into the path between the waveguide oscillator and the bolometer. By varying the separation of mirrors of the spectrometer over a distance of about 5 cm, we were able to determine the wavelength to an accuracy of about 0.1%.

The highest power density obtained with GaAs/AlAs and InAs/AlSb RTDs in each of these resonators is shown in Fig. 5. At 360 GHz, the InAs/AlSb RTD produced a power density of about  $90\text{ W cm}^{-2}$  and an absolute power of  $3\text{ }\mu\text{W}$ . This is 50 times the power density obtained from GaAs/AlAs diodes at 370 GHz. In the WR-1 resonator, the highest power was  $0.3\text{ }\mu\text{W}$ , which was obtained from a  $1.8\times 1.8\text{-}\mu\text{m}$  InAs/AlSb RTD oscillating at 712 GHz. This corresponds to a power density of  $15\text{ W cm}^{-2}$ . Our uncertainty in these values is about 75%, reflecting the great difficulty in calibrating power measurements in this frequency region. To determine whether the 712-GHz signal resulted from a fundamental oscillation or a harmonic of a lower frequency oscillation, we used the Fabry-Perot spectrometer to look for changes in the oscillation frequency with variations in position of the backshort. We found that the backshort tuned the output frequency by about 2 GHz. This tuning would probably not be observed if the oscillation were a harmonic, since propagation at the fundamental frequency could not occur in the waveguide, and thus the oscillation frequency would not depend on the backshort position. However, harmonic-tuning effects cannot be completely ruled out, and better techniques are needed for this determination.

### Quasioptical resonator performance

A major challenge in operating solid-state oscillators at frequencies above 100 GHz is the design of the resonator. Conventional resonators, such as those based on closed cavities or radial transmission lines, exhibit an unloaded quality factor  $Q_u$  that decreases with increasing frequency because of increases in the ohmic and scattering losses of metallic surfaces. Open resonators, such as those used in lasers, provide a much higher  $Q_u$  but are difficult to integrate with lumped-element, solid-state oscillators. We have combined a waveguide RTD oscillator and a high- $Q_u$  semiconfocal cavity to form a quasioptical oscillator operating at frequencies near 100 GHz. With no electromagnetic coupling between the waveguide and the semiconfocal cavity, the oscillator power was approximately  $10\text{ }\mu\text{W}$  and the 10-dB-down linewidth was 10 MHz. With coupling to the cavity, the oscillator power decreased by about 3 dB and the linewidth decreased to roughly 40 kHz. Accompanying this reduction in linewidth was a locking of the oscillator output onto a semiconfocal-cavity mode. Our

technique provides a sufficiently narrow linewidth for local-oscillator applications in radiometers.

The schematic diagram of our quasioptical oscillator designed for the 100-GHz region is shown in Fig. 6. The RTD is mounted in a standard-height rectangular waveguide in the manner used in all of our waveguide RTD oscillators operating above 100 GHz. The diode is dc biased by a coaxial circuit that suppresses spurious oscillations by means of a very lossy section of transmission line placed in close proximity to the top wall of the waveguide. The waveguide section opens abruptly within the middle of a flat metallic wall that forms one reflector of a semiconfocal open resonator. The  $TEM_{00N}$  modes of this resonator are assumed to have a Gaussian transverse intensity profile with  $1/e$ -point loci as shown in Fig. 6. The spot diameter of these modes at the flat reflector are designed to be about 10 times the height of the rectangular waveguide. This large spot diameter (the radiation pattern from the end of the waveguide is actually more divergent than a Gaussian mode) makes the coupling between the waveguide and the open cavity fairly weak. Weak coupling is necessary to realize a large  $Q_u$  for the open resonator. The output radiation of the oscillator is taken from the opposite end of the waveguide section. The power of the oscillator is measured by a Schottky-diode detector and the spectrum is resolved by down-converting the oscillator output to the frequency range of a microwave spectrum analyzer.

Experimental power spectra of the RTD oscillator are shown in Fig. 7. The broad spectrum in Fig. 7(a) results from the insertion of an absorbing element into the open resonator that spoils the  $Q_u$ . In this case, the oscillation is based on the waveguide LC resonance discussed previously. The width of the spectrum is roughly 10 MHz, which is unsuitable for local-oscillator applications. Upon removing the absorber, the spectrum shifts and becomes much narrower. The expansion of this spectrum, shown in Fig. 7(b), yields a linewidth of about 40 kHz. The shift in frequency is a result of the RTD oscillation being locked onto the open-cavity resonance. The narrowing is a further indication that locking has occurred and is consistent with the high  $Q_u$  of the open resonator compared to that of the waveguide resonance. The center frequency of the cavity resonance is determined, as in all Fabry-Perot resonators, by the spatial separation of the reflectors. By varying this separation, we were able to tune the locked power spectrum over a range of about 0.3 GHz at a fixed RTD bias voltage. We are presently determining the effect of the open cavity for different RTD bias voltages. For the waveguide oscillator, the center frequency could be tuned by roughly 10 GHz with variation of RTD bias voltage.

The power of the cavity-locked oscillation in Fig. 7(a) (the integral under the power spectrum) was found to be about 3 dB less than the unlocked power of approximately 10  $\mu$ W. One could obtain significantly more power and maintain the advantage of quasioptical locking by implementing an array of RTD oscillators rather than the single-element oscillation demonstrated here. In principle, such an array could consist of a parallel combination of waveguide-mounted RTD structures like that shown in Fig. 6. However, a more practical approach for very high frequencies is a planar RTD array based on microstrip-circuit

techniques. The key point in either approach is that the oscillators all lie in an equiphase plane of the open-cavity mode and are thus synchronized by the high- $Q_u$  resonance. This method of power combination has been used to obtain cw power levels up to 20 W from both planar-MESFET oscillator arrays and Gunn-diode oscillator arrays operating near 10 GHz.<sup>5</sup> It should be a useful technique for obtaining milliwatt levels of power from RTD oscillators in the submillimeter-wave region.

### Summary

InAs/AlSb RTDs have oscillated up to 712 GHz at room temperature. The power density generated at lower frequencies is 50 times that obtained from the best GaAs/AlAs RTD at the same frequency. The superiority of the InAs/AlSb RTD stems from its superior ohmic contact and from its higher available current density. A semiconfocal resonator has been used to lock a waveguide-based RTD oscillator at a frequency of 103 GHz. The locked oscillator linewidth was 40 kHz, which is about 250 times narrower than the linewidth of the waveguide oscillator alone. The quasioptical RTD oscillator should be suitable as a local oscillator for superconducting tunnel-junction mixers up to frequencies of at least 400 GHz.

### Acknowledgments

The authors are grateful to A.R. Calawa and M.J. Manfra for providing the  $\text{In}_{0.53}\text{Ga}_{0.47}\text{As}/\text{AlAs}$  materials, to J.R. Söderström, S.J. Eglash, and T.C. McGill for providing the InAs/AlSb materials, to L.J. Mahoney and C.L. Chen for fabrication support, to D.L. Landers for valuable assistance in dicing and packaging, to R.A. Murphy and M.A. Hollis for useful comments on the manuscript, and to A.L. McWhorter for theoretical advice and useful comments on the manuscript. This work was sponsored by NASA through the Jet Propulsion Laboratory, by the Air Force Office of Scientific Research, and by the U.S. Army Research Office.

### References

1. E.R. Brown, T.C.L.G. Sollner, C.D. Parker, W.D. Goodhue, and C.L. Chen, *Appl. Phys. Lett.* **55**, (1989), p. 1777.
2. E.R. Brown, C.D. Parker, A.R. Calawa, M.J. Manfra, T.C.L.G. Sollner, C.L. Chen, S.W. Pang, and K.M. Molvar, *Proc. SPIE* **1288**, (1990), p. 122.
3. J.R. Söderström, E.R. Brown, C.D. Parker, L.J. Mahoney, and T.C. McGill, *Appl. Phys. Lett.* **58**, (1991), p. 275.
4. P. Boher, M. Renaud, J.M. Lopez-Villegas, J. Schneider, and J.P. Chane, *Appl. Surf. Sci.* **30**, (1987), p. 100.
5. D.B. Rutledge, Z.B. Popovic, R.M. Weikle, M. Kim, K.A. Potter, R.C. Compton, and R.A. York, *1990 IEEE MTT-S Int. Microwave Symp. Digest*, p. 1201.

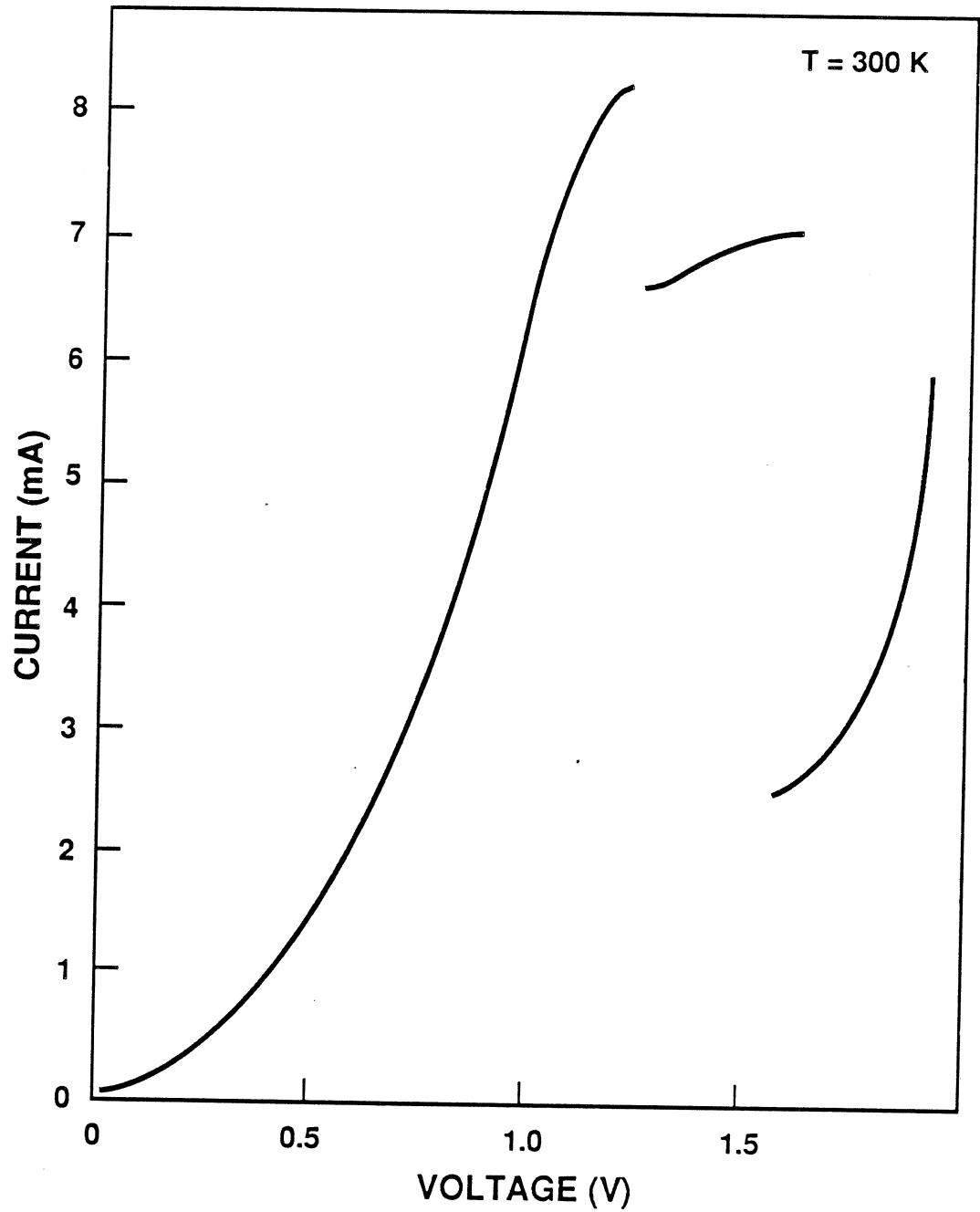


Fig. 1. I-V characteristics of a 1.8- $\mu\text{m}$ -diameter InAs/AlSb RTD at room temperature. The step structure spanning the NDC region is caused by self-rectification of the oscillations.

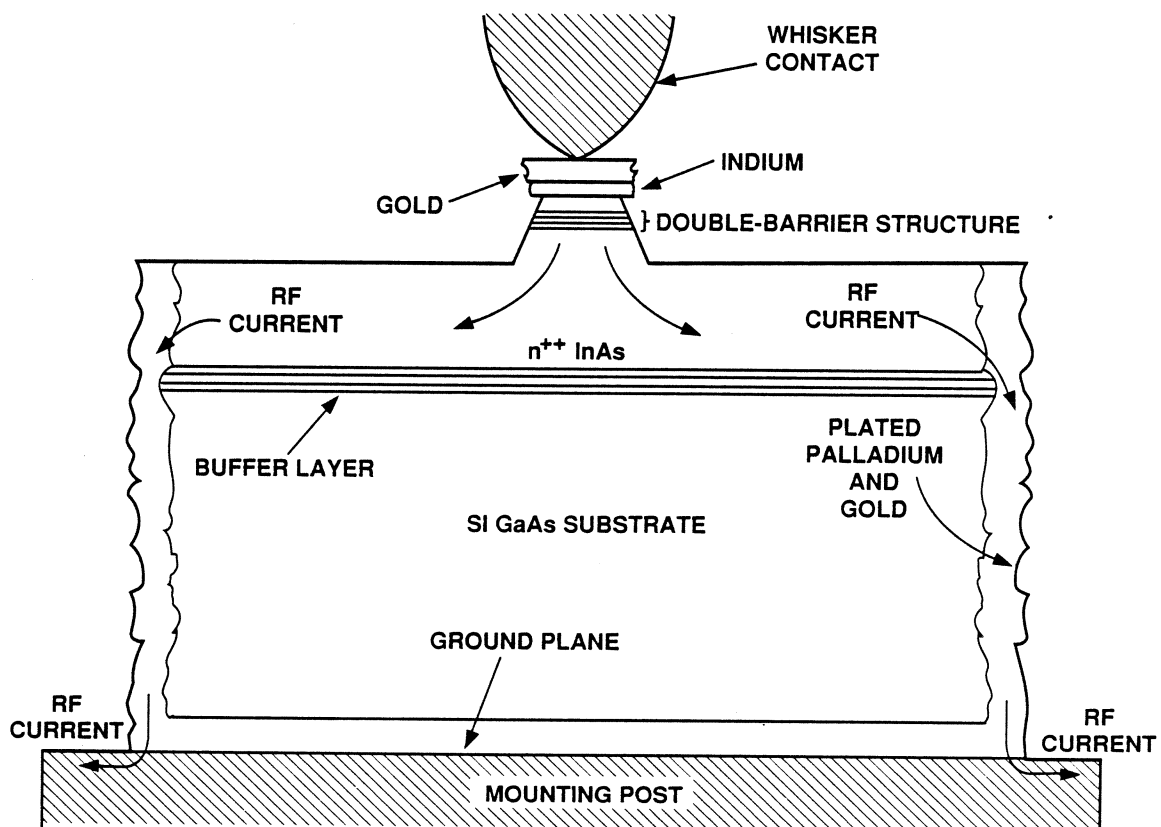


Fig. 2. Cross-sectional view of a fabricated InAs/AlSb RTD chip showing the current path followed between the diode mesa and the ground plane.

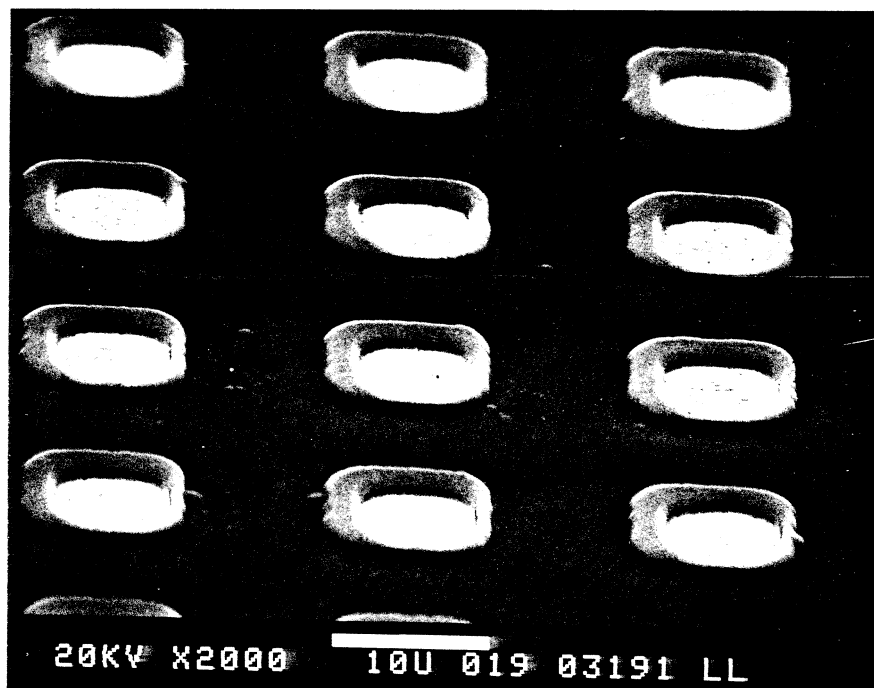


Fig. 3. Honeycomb pattern fabricated on top surface of RTD chip. The light regions are gold contacts on top of InAs mesas. The dark region is where a 1.0- $\mu\text{m}$ -thick layer of  $\text{Si}_3\text{N}_4$  covers etched InAs.



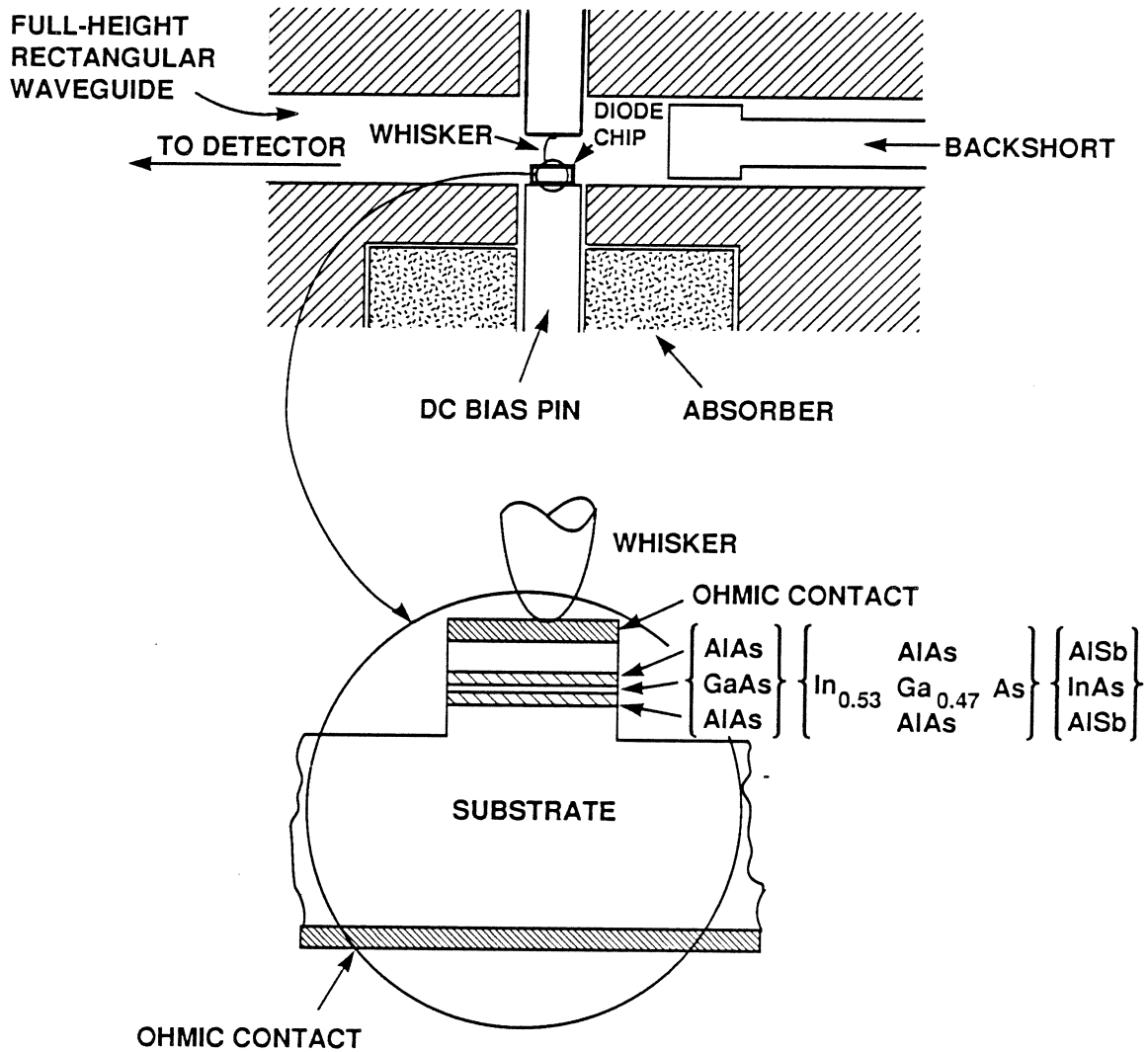


Fig. 4. Schematic diagram of waveguide resonator used to study RTD oscillators at frequencies above 100 GHz. The inset shows a cross-sectional view of a whisker-contacted RTD.

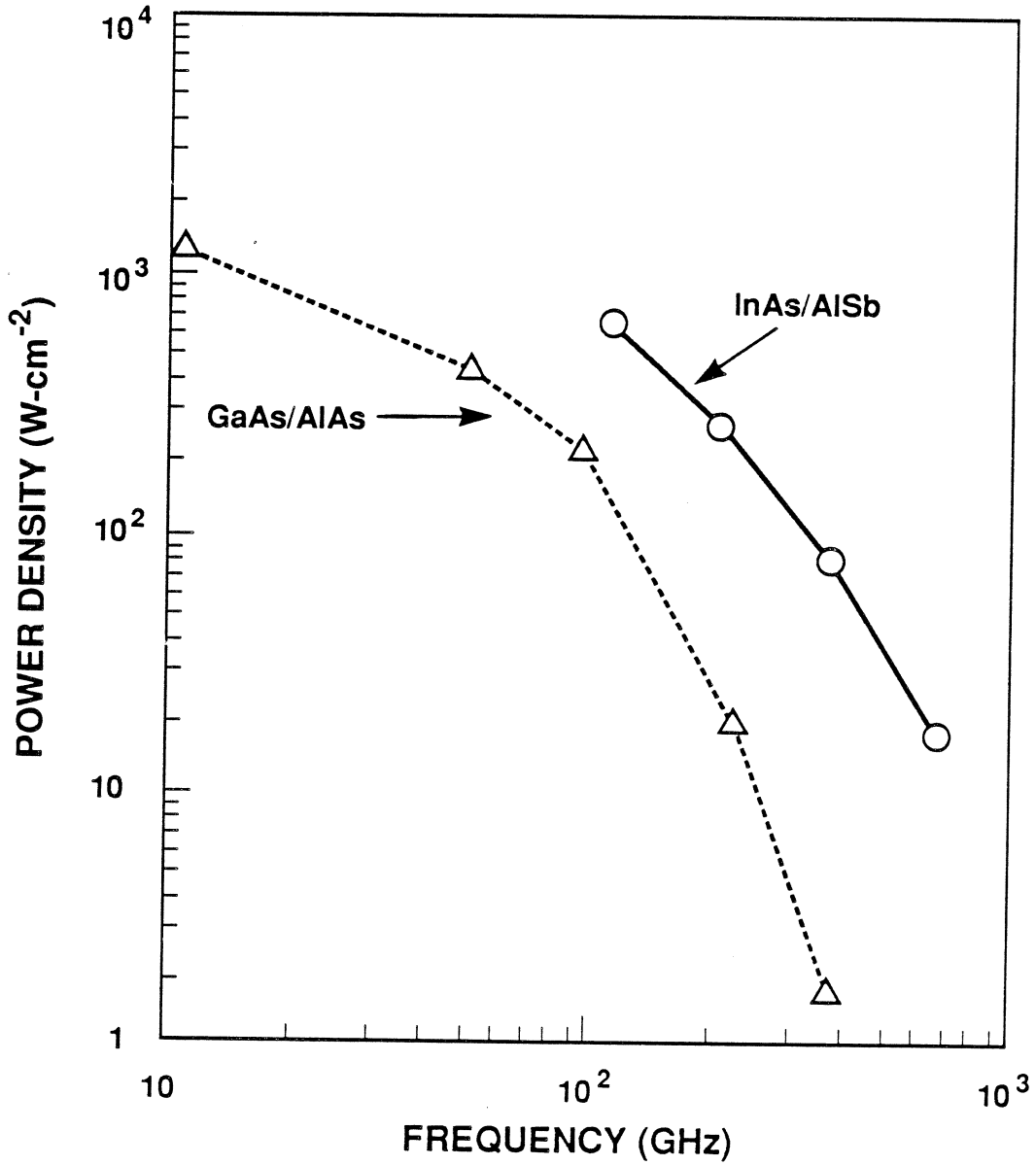


Fig. 5. Oscillator results for GaAs/AlAs and InAs/AlSb RTDs at room temperature.

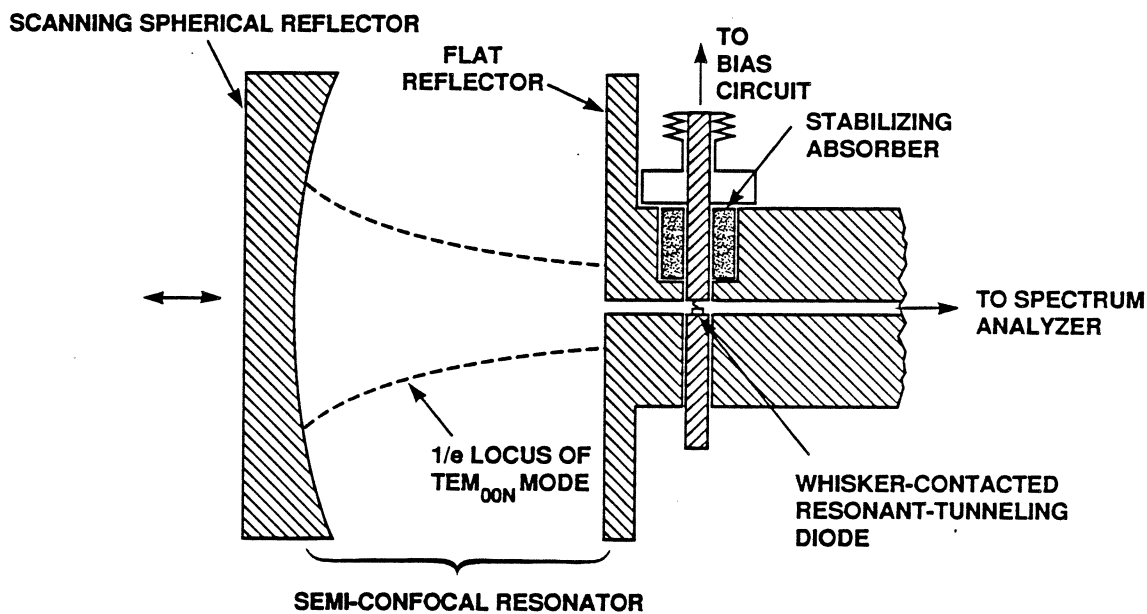


Fig. 6. Schematic diagram of quasioptical RTD oscillator designed to operate in the 100-GHz region.

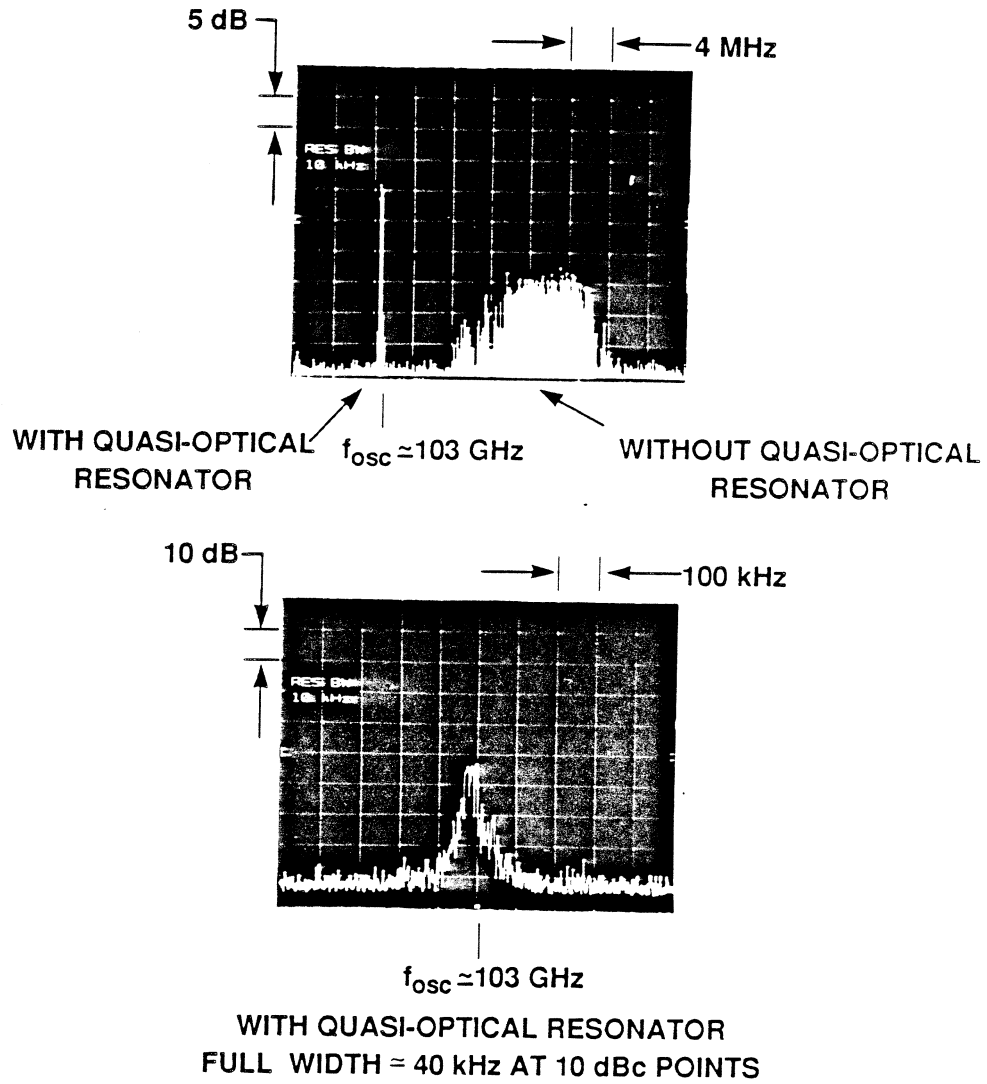


Fig. 7. (a) Power spectrum of the quasi-optical oscillator with and without the benefit of the semiconfocal open resonator. (b) Expansion of the frequency axis of the power spectrum measured with the semiconfocal open resonator.